Available free online at www.medjchem.com

Mediterranean Journal of Chemistry

Mediterranean Journal of Chemistry **2020**, 10(4), 310-318

A sol-gel synthesis, characterization and *in vitro* bioactivity of binary, ternary and quaternary bioglasses with high mechanical strength

Sarra Bouhazma [1], Imane Adouar [1], Sanae Chajri [1], Smaiel Herradi [1], Mohamed Khaldi [1], Abdelkrim Ouammou [1], Brahim El Bali [1], Mohammed Mansori [2] and Mohammed Lachkar [1, *]

[1] Engineering Laboratory of Organometallic and Molecular Materials and Environment, Faculty of Sciences, University Sidi Mohamed Ben Abdellah, 30000 Fez, Morocco

[2] Laboratory of Chemistry of Materials and Environment, Faculty of Sciences and Technology, University Cadi Ayyad, Po. Box 549, Gueliz Marrakech, Morocco

Abstract: Bioactive powders of the binary SiO_2-CaO, ternary SiO_2-CaO-P_2O_5 and quaternary systems SiO_2-CaO-P_2O_5-Na_2O/Mg_2O were synthesized using a sol-gel route. The gels were converted into bioglasses powders by heat treatments at the temperature of 700°C. The resulting materials were characterized by X-ray diffraction (XRD), Fourier Transform Infrared spectroscopy (FTIR), Environmental Scanning Electron Microscopy (ESEM) and *in vitro* bioactivity in acellular Simulated Body Fluid (SBF). The *in vitro* tests showed that the samples had the good apatite-forming ability. Glasses doped with sodium and magnesium show good results in terms of bioactivity and mechanical properties. The results showed that the quaternary glass SiO_2-CaO-P_2O_5-Na_2O containing Na is the most bioactive, only 6 hours after its immersion in SBF; a layer of hydroxycarbonated apatite (HAC) was deposited on the glass and compressive strength of up to 233.08 MPa with a porosity of 11.02%, due to the presence of the $Na_2Ca_2Si_3O_9$ phase. Magnesium also affects bioactivity because it has improved from binary to ternary to quaternary doped with magnesium, bioactive from 12h of contact with the SBF.

Key words: Binary, ternary and quaternary bioglasses; sol-gel; in vitro bioactivity; mechanical strength, porosity, orthopaedics.

1. Introduction

Bioglasses and glass-ceramics have received particular interest due to their unique characteristics [1]. Bioactive glasses in the system SiO_2-CaO-P_2O_5-Na_2O have been shown to form a mechanically strong bond to bone and too soft tissues; bonding occurs by the rapid formation of a thin layer of hydroxycarbonate apatite (similar to biological apatite) on the glass surface when implanted or in contact with biological fluids [2, 3]. They can be synthesized by traditional melt quenching or by the versatile sol-gel process [4, 5]. Furthermore, bioglasses prepared via sol-gel method always have an interconnected mesoporous structure and a higher reactive surface, allowing better nucleation of the hydroxycarbonate apatite during the soaking of the material *in vitro* or *in vivo* [6]. Glass formers were chosen based on previous studies in the field of sol-gel bioglasses [7]. Different dopants were selected such as sodium and magnesium. Magnesium is essential to bone metabolism, and it has been shown to have stimulating effects on new bone formation [8]. Magnesium is suggested to interact with integrins of osteoblast cells, which are responsible for cell adhesion and stability [8, 9]. Rude *et al.* [10, 11] observed that magnesium depletion results in impaired bone growth, increased bone resorption and loss in trabecular bone underlining the significant role that magnesium plays in bone metabolism. The formation of $Na_2Ca_2Si_3O_9$ [12] in the bioglass doped with sodium significantly improves the mechanical properties of the material; crystallization does not inhibit bioactivity, with the bone-bonding ability (indicated by the formation of hydroxyapatite) remaining in the fully crystallized ceramics. When immersed in body fluid, the crystalline phase $Na_2Ca_2Si_3O_9$ decomposes and transits to amorphous hydroxyapatite (HA), an easily degradable mineral *in vivo*. The presence of Na_2O offers advantages in relation to the crystallization treatment that is applied to improve the mechanical properties of bioceramics. Because scaffolds of amorphous bioactive glasses are very fragile, to achieve superior mechanical

*Corresponding author: Mohammed Lachkar
Email address: lachkar.mohammed@gmail.com
DOI: http://dx.doi.org/10.13171/mjc02003141026lea

Received August 31, 2019
Accepted Octobre 22, 2019
Published April 13, 2020

strength bioactive glass foams have to be sintered to form crystalline phases [12]. In bioactive glasses lacking Na_2O the crystalline phase is bioinert [13], which means that mechanical strength is improved, at the cost of sacrificing degradability. Despite the vast literature describing the mechanical properties of different types of glass-ceramics [14, 15], there are only a few studies concerned with bioactive glass-ceramics, and particularly for this family of highly bioactive glass-ceramics. Several studies have compared the mechanical behavior of the parent glasses with fully crystallized glass-ceramics but without consideration the porosity. Others have compared the mechanical behavior of glass-ceramics with varying crystal size for a fixed volume percentage of crystal phase. Indeed, in the present work, we independently studied one microstructural factor that affects the mechanical behavior of the material: the porosity of each glass, the results are in agreement with the already reported by Chajri *et al.* [16]. In the present study and as a continuation of our recent published investigations in these systems [16, 17]; it was decided to use the sol-gel process for the synthesis with an acid catalyst. First, the choice of the studied compositions is explained, and then the paper summarizes the sol-gel process and the treatment to obtain the glasses. A comparison is made between the glasses (SiO_2-CaO-P_2O_5-MgO (7.5Mg), SiO_2-CaO (77b), a ternary SiO_2-CaO-P_2O_5 (57t) and a quaternary SiO_2-CaO-P_2O_5-Na_2O (24Na) bioglasses) obtained by the sol-gel explaining the role of each element doped in the glasses, namely sodium and magnesium.

2. Experimental

2.1. Sample synthesis

2.1.1. Selection of compositions

The compositions were chosen based on previous studies [18, 19]. Initially, we based our selves on the Hench triangle, and we created a series of compositions for each type of glass (binary, ternary and quaternary system), to finally optimize the glass that has the best bioactivity. Then the properties of the binary and ternary glasses obtained by sol-gel route were compared with quaternary glasses doped by sodium and magnesium. The composition of the systems is listed in Table 1.

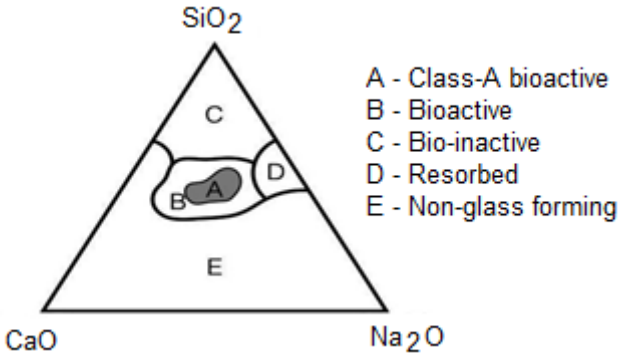

Figure 1. Property changes of bioglass materials [20].

Table 1. Composition (mol %) of sol-gel glasses.

Samples	SiO_2	CaO	P_2O_5	MgO	Na_2O
77b	77	23	0	0	0
57t	57	33	10	0	0
24Na	46	24	6	0	24
7.5Mg	50	32.5	10	7.5	0

2.1.2. Synthesis by sol-gel

The bioglasses 77b, 57t, 7.5Mg, and 24Na were synthesized by a sol-gel technique and characterized for their physicochemical properties. In the first step, the solution was prepared as follows: 12 g of the tetraethylorthosilicate (TEOS; Merck) $Si(C_2H_5O)_4$ was added into 30 mL of 0.1 M nitric acid; the mixture was allowed to react for 30 min for the acid hydrolysis of TEOS to proceed almost to completion. The following reagents were added in sequence allowing 45 min for each reagent to react completely: 0.89 g (0.005 mol) triethylphosphate (TEP), 5.16 g (0.026 mol) of calcium nitrate tetrahydrate, and 1.68 g (0.005 mol) of magnesium nitrate hexahydrate. After the final addition, mixing was continued for 1 h to allow completion of the hydrolysis reaction. The solution was cast in a cylindrical Teflon container and kept sealed for 10 days at room temperature to let the hydrolysis and a polycondensation reaction to take place until the gel was formed. The gel was held in a sealed container and heated at 70°C for 3 days. To get rid of the water, a small hole was contrived in the lid to allow the leakage of gases while heating the gel to

150°C for 52 hours to remove all the water. The dried gel was then heated for 3h at 700°C for two reasons; first to stabilize the glass and second to eliminate residual nitrate [21].

2.2. Characterizations of the samples

2.2.1. FT-IR analysis

Fourier transform infrared spectroscopy (FTIR: Bruker VERTEX 70 spectrometer) was used to analyze the functional group of the obtained powders. The spectra were recorded from 400 to 4000 cm^{-1} at 4 cm^{-1} resolution.

2.2.2. XRD analysis

The characterization of the crystalline resulting phases, before and after immersion in SBF, was performed by XRD. X-ray diffraction measurements were presented with a Discover model operated at 40 kV and 40 mA using Cu-K_α radiation (λ = 1.5418 Å) in the range (10-80°) and step size of 0.02° and a step duration of 2s.

2.2.3. ESEM analysis

Morphological characterization of the pellets regarding the surface modifications that occurred during the *in vitro* bioactivity tests was performed by ESEM. A set of samples was selected and analyzed, using a scanning electron microscopy coupled with energy-dispersive spectroscopy: ESEM Quanta 200 (FEI Company).

2.3. *In vitro* test

The bioactivity evaluation was realized through immersion of each sample in a polystyrene bottle containing 45 mL of Simulated Body Fluid (SBF), maintained at 37 ± 0.5°C for 6 to 240 hours. After soaking, the sample was filtered and dried in air. The SBF solution was prepared by dissolving reagent grade chemicals of NaCl, $NaHCO_3$, KCl, $K_2HPO_4.3H_2O$, $MgCl_2.6H_2O$, $CaCl_2.2H_2O$ and Na_2SO_4 into distilled water (Table 3) and buffered at pH 7.42 with 50 mM tris(hydroxymethyl)-aminomethane and 45 mM HCl [22]. SBF is known to reproduce hydroxycarbonated apatite (HCA) formation on the surface of bioactive glasses and glass-ceramics by simulating the reaction occurring in the human body (Table 2). It is essential to mention that this solution is often used in the *in vitro* evaluation of the formation of a hydroxycarbonated apatite layer on the surface of materials designed for implants, according to ISO23317, approved in June 2007 by the International Organization for Standardization [23].

Table 2. Ion concentrations (mM) of SBF and human blood plasma [22].

Ion	Simulate Body Fluid	Blood plasma
Na^+	142.0	142.0
K^+	5.0	5.0
Mg^{2+}	1.5	1.5
Ca^{2+}	2.5	2.5
Cl^-	148.8	103.0
HCO_3^-	4.2	27.0
HPO_4^{2-}	1.0	1.0
SO_4^{2-}	0.5	0.5

Table 3. Reagents for preparing the SBF.

Order	Reagent	Amount
1	NaCl	7.996 g
2	$NaHCO_3$	0.350 g
3	KCl	0.224 g
4	$K_2HPO_4 \cdot 3H_2O$	0.228 g
5	$MgCl_2 \cdot 6H_2O$	0.305 g
6	1M-HCl	40 mL
(About 90% of total amount of HCl to be added)		
7	$CaCl_2$	0.278 g
8	Na_2SO_4	0.071 g
9	$(CH_2OH)_3CNH_2$	6.057 g

2.4. Mechanical strength of synthesized bioglasses

Despite the fact that there is a growing interest in bioactive glass and derived glass-ceramic structures [24] and their in vitro and in vivo properties are well documented [25], few studies that have studied their mechanical strength have only discussed compressive strength, [26, 27] because compressive strength is the ability of a material to withstand vertically applied pressure forces without sustaining excessive longitudinal or transverse deformation. In contrast to metals and plastics, bioglasses are not very elastic. Their mechanical rigidity differentiates them from these materials, which is generally seen as an advantage for their use in harsh environments. The compressive strength measurements were carried out on a universal testing machine; model INSTRON 3369, equipped with a 2.5 kN load cell. Specific attention was paid to the good parallelism between the flat surfaces under compression. The testing speed was set at 0.1 mm/min. The samples were cylindrical in shape, sintered, with standard dimensions: 20 mm in height and 10 ×10 mm in cross-section. During compression, testing the load was applied until densification of the porous samples started to occur. Three tests were performed on each sample to establish an average.

2.5. Study of porosity

To try to quantify of the total porosity of the bioglass, a measurement of the relative density in an aqueous medium is made; the bulk density and open porosity of the samples were determined by the method of Arthur [28]. The total porosity can be calculated if the theoretical density of the material is known. We weigh the sample in air (m_1). It is then placed on a support in a vacuum desiccator containing xylene. Allowed the sample 2h under vacuum to degas, then it is dipped in xylene to ensure thorough penetration of the impregnating liquid into the open pores. Finally, the impregnated sample is then weighed again (m_2), then water (m_3).

3. Results and Discussion

X-ray diffraction and FTIR evidenced the formation of an apatite-like layer on the glasses surface after soaking in SBF. Figure 2 shows the X-ray diffraction analysis of the four glasses 77b, 57t, 24Na and 7.5Mg before soaking in SBF. XRD spectra were generated from the whole material of the powder used, rather than from a surface layer of powder particles. Hence, the spectra obtained represent the structure throughout the material. Bioglasses 77b, 57t, and 7.5Mg are amorphous, while the crystalline phase $Na_2Ca_2Si_3O_9$ was identified in the as-sintered 24Na powder.

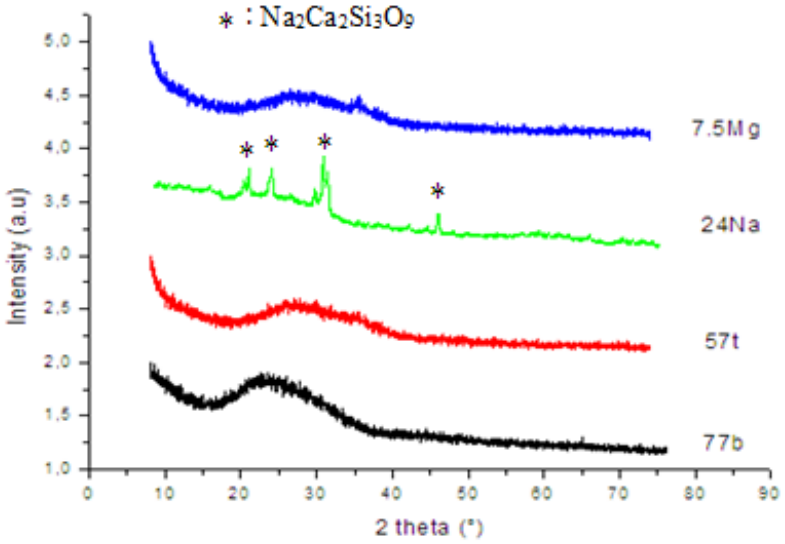

Figure 2. XRD spectra of sol-gel derived 77b, 57t, 24Na and 7.5Mg glass-ceramics after heated at 700°C for 3h.

All glasses are bioactive by different times, the patterns obtained for the glasses after soaking don't exhibit peaks characteristic of hydroxyapatite. Compared with the amorphous structure before immersion, after 2 days of soaking, the XRD pattern of sample sintered at 700°C showed a wide diffraction peak corresponding to (211) reflections of an apatite phase (Figure 3(a)).

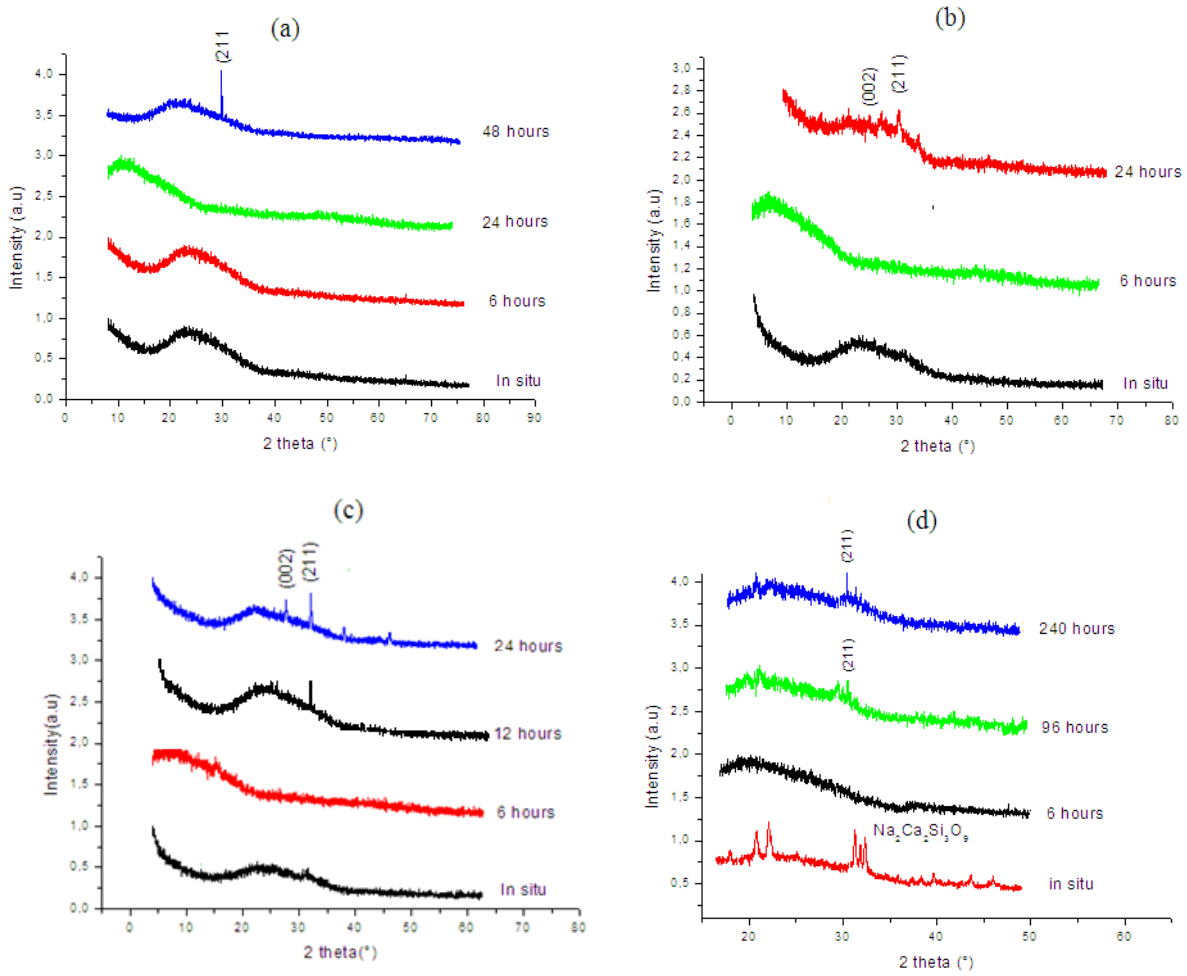

Figure 3. XRD spectra of the sol-gel derived bio-glasses (heated at 700°C/3h) before and after immersion in SBF for different times. (a) 77b, (b) 57t, (c) 7.5Mg, (d) 24Na.

Bioglass 57t is more bioactive than the bioglass 77b. Figure 3(b) shows diffraction peaks corresponding to the (002) and (211) reflections of calcium phosphate carbonate hydroxide [$Ca_5(PO_4,CO_3)_3(OH)$] after 24 hours of immersion in SBF. The quaternary systems 24Na and 7.5Mg are bioactive, but both elements behave differently. Various studies have investigated magnesium-containing polycrystalline ceramics and material glass-ceramics for biomedical applications [29-31]. Notably, the Mg may be able to enter the forming hydroxyapatite nuclei and thus inhibits their evolution to tiny apatite crystals, because this element cannot be accommodated in the hydroxyapatite structure. Mg^{2+} substitute into the apatite lattice, which causes changes in its physicochemical properties. Apatite substituted with Mg results in a calcium-deficient apatite and may be amorphous calcium phosphate (Ca, $Mg)_9(PO_4)_6$ [32, 33]. The higher the MgO content of the glasses, the lower is the rate of the calcium phosphate layer formation and the higher is the thickness of this layer [34]. The substance formed on glasses became detectable after 12 hours immersion in SBF, a new peak at 32° were assigned to be (211) apatite according to the standard JCPDS cards (09-0432) [Figure 3(c)] [35].

Moreover, after 1 day of immersion, the one peak was intensified, and the other peak of apatite at 26° appeared. The XRD pattern shows some wide hydroxyapatite reflection, indicating a poor crystalline phase formation [36]. However, these results are in disagreement with those gotten when using the sol-gel made 45S5 bioglass [37]. 7.5Mg bioglass behaves like 45S5 bioglass® synthesized by melting method, both bioactive after 12 hours, while the sol-gel 45S5 is active after 15 days. XRD data of the glass surface versus time are presented on Figure 3(d) for the unsoaked sample. The XRD data emphasized the predominant amorphous feature of the sample 24Na. The diffraction peaks of the $Na_2Ca_2Si_3O_9$ phase became shorter with increasing incubation time in SBF, eventually disappearing after incubation for 6 h. After 96 h, a broad halo pattern (indicating an amorphous structure) overlaid with small apatite peaks; this result is in agreement with the results published by Bouhazma *et al.* [17]. After 6 h of soaking in the SBF, the recorded diagram revealed the presence of a well-crystallized hydroxyapatite phase.

Figure 4 shows the FTIR spectra of samples before

soaking in SBF. Before soaking, the spectra of the sample exhibited Si–O–Si stretching and bending bands. The band at around 1080 cm^{-1} corresponds to the vibrational mode of the asymmetric stretch of Si–O–Si, the band at 800 cm^{-1} corresponds to the symmetric stretch of Si–O, and the strong band at 475 cm^{-1} corresponds to the vibrational mode of the bending of Si–O–Si. After soaking at various times, additional peaks appeared around 550-600 cm^{-1}: the twin bands at 570 cm^{-1} and 600 cm^{-1} (P–O bands) which correspond to antisymmetric vibration mode of P–O in amorphous calcium phosphate, the band at 1430 cm^{-1} corresponds to carbonate and 3457 cm^{-1} corresponds to H_2O, all bands indicate apatite formation in SBF [38, 39]. These data confirm the XRD findings.

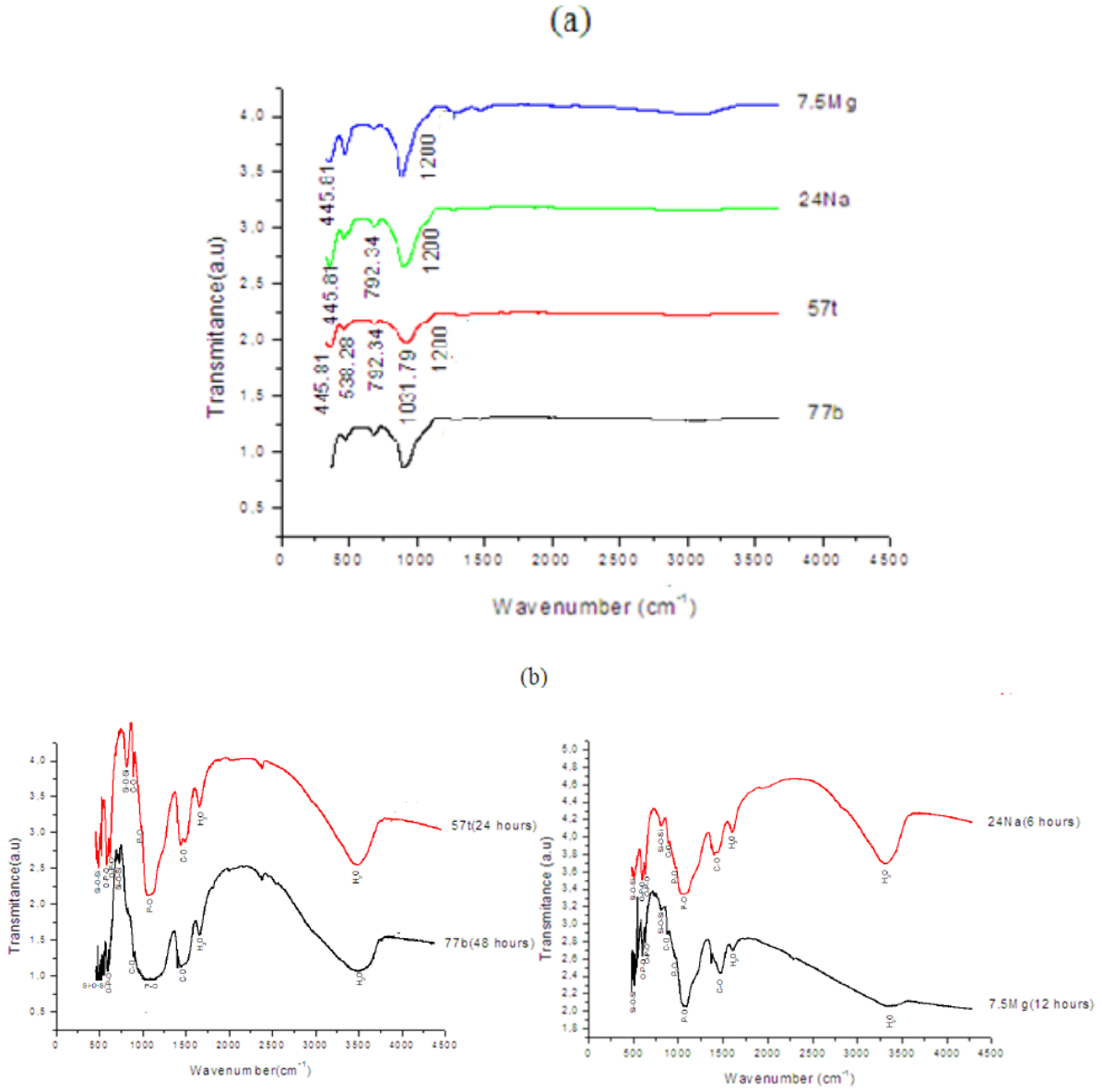

Figure 4. Fourier transform IR spectra obtained for glasses 77b, 57t, 24Na, and 7.5Mg before and after immersion in SBF for different times: (a) before, (b) after.

ESEM micrographs showing the structures of the glasses 77b, 57t, 7.5Mg, and 24Na are depicted in Figure 5. Bioglasses 77b and 57t have almost the same structure, both composed of irregular particles. 7.5Mg gel glass reveals a difference in morphology; its surface is wrinkled. For 24Na, we could also observe that the surface was covered with semispherical particles. These observations will be confirmed by the study of mechanical strength and porosity.

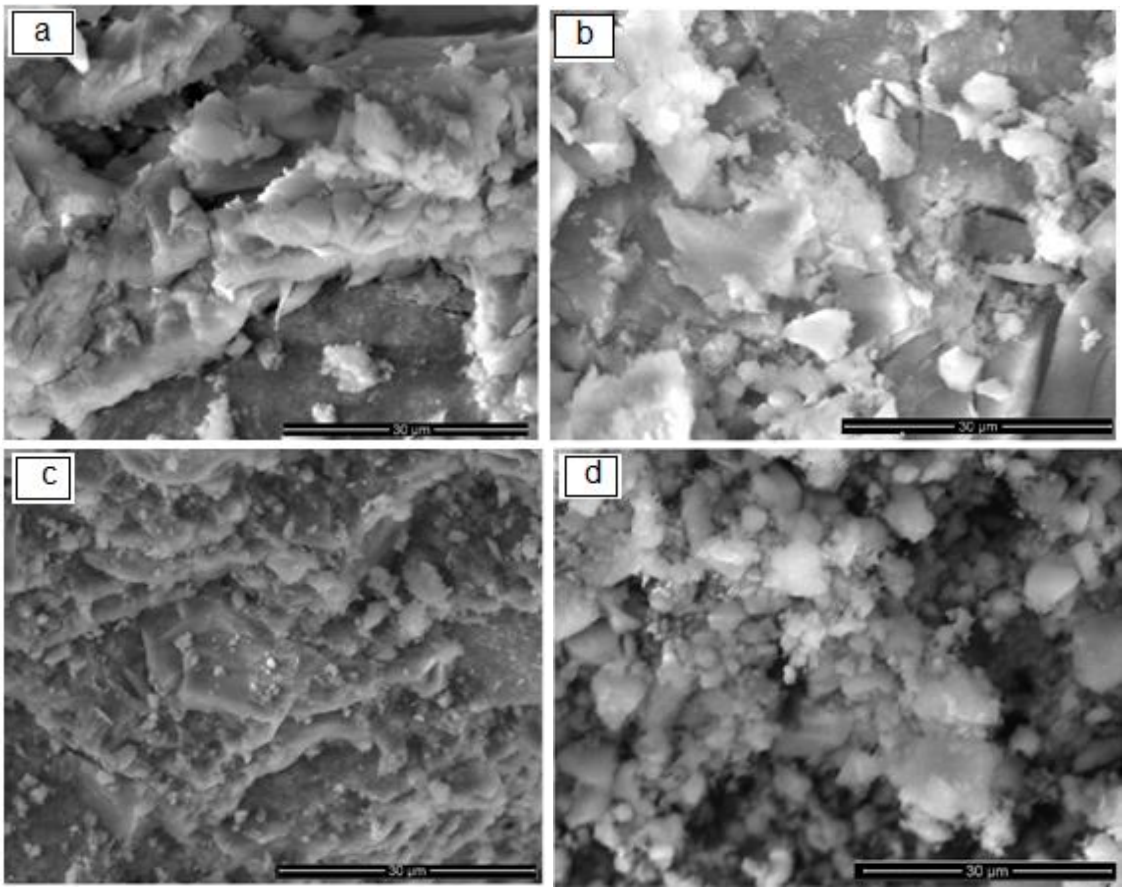

Figure 5. ESEM morphology of the sol-gel derived bioglasses powder: (a) 77b, (b) 57t, (c) 7.5Mg, (d) 24Na.

From an engineering point of view, it is desirable to select the scaffold material taking into account the mechanical parameters of the tissue of concern. Generally, two ways are considered: the selection of the material to have a perfect match of mechanical parameters; admittance of some variations of the mechanical parameters within a suitable tolerance range. Table 4 summarizes the mechanical properties of human cancellous and cortical bone, comparing them to dense 45S5 Bioglass [40].

Table 4. Mechanical properties of trabecular and cortical bone compared to 45S5 BG composition data from [40].

Material Property	Trabecular Bone	Cortical Bone	45S5 Bioglass
Compressive Property (MPa)	0.1-16	130-200	500
Porosity (%)	50-90	5-10	4-10

Table 5. Mechanical property and porosity of glasses 77b, 57t, 7.5Mg and 24Na.

Samples	77b	57t	7.5Mg	24Na
% of porosity	41.18 ± 0.25	30.38 ± 0.15	15.05 ± 0.35	11.02 ± 0.05
Compressive strength values (MPa)	61.33 ± 0.26	89.25 ± 0.21	161.16 ± 0.11	233.08 ± 0.05

Table 5 shows the compressive strength and porosity of the synthesized glasses. The mechanical properties were improved by incorporating Na_2O into bioactive glasses [12], which can result in the formation of a hard yet biodegradable crystalline phase from sintered bioactive glasses. It can be seen that the mechanical strength and the porosity were inversely proportional. This result is in good agreement with previous reports like in porous structures showing indirect relationships between porosity and mechanical strength [41]. In our case, with the improvement of porosity from 11.02 to 41.18%, the mechanical strength reduced from 233.08 to 61.33 MPa. These results are to compare to what was reported for porous structures, an increase of porosity from 63.5 to 90.3%, leading to a decrease of the mechanical strength from 1.13 to 0.53 MPa [42]. One can conclude that the glass has excellent mechanical strength because the surface is homogenous [43].

4. Conclusion

All the gel glasses studied in the binary, ternary and quaternary systems are bioactive and form a hydrated carbonate apatite layer on their surface on exposure to SBF. Incorporation of P, Mg, and Na into a bioglass system does not diminish the bioactivity of such material. The presence of phosphorous, magnesium and sodium in the composition of the glass has produced the following effects: it slows down the rate of formation of the apatite layer, the glass 77b present the important porosity (41.18%) that is why the mechanical strength is modest. This property is improved by incorporating Na_2O into bioactive glasses with medium porosity (11.02%). The results showed that 24Na glass is the most bioactive (after 6 hours of immersion in SBF, a layer of HAC was deposited on the glass) and compressive strength of up to 233.08 MPa with a porosity of 11.02%. The composition, bioactivity, the porosity, and the mechanical properties make the bioglass 24Na a potential candidate for tissue repair and tissue engineering applications.

Acknowledgements

The authors would like to acknowledge the support and technical assistance of Interface Regional University Center (Sidi Mohammed Ben Abdellah University, Fez), and National Center for Scientific and Technical Research (CNRST-Rabat).

References

1- F. Baino, G. Novajra, C. Vitale-Brovarone, Bioceramics and scaffolds: A winning combination for tissue Engineering, Front. Bioeng. Biotechnol., **2015**, 3, 1-17.
2- F. Baino, C. Vitale-Brovarone, Three-dimensional glass-derived scaffolds for bone tissue engineering: Current trends and forecasts for the future, J. Biomed. Mater. Res. A., **2011**, 97, 514-535.
3- Q. Fu, E. Saiz, A.P. Tomsia, Direct ink writing of highly porous and strong glass scaffolds for load-bearing bone defects repair and regeneration, Acta Biomater., **2011**, 7, 3547-3554.
4- L. L. Hench, J. R. Jones, Bioactive glasses: Frontiers and challenges, Front. Bioeng. Biotechnol., **2015**, 3, 194.
5- V. Miguez-Pacheco, L. L. Hench, A. R. Boccaccini, Bioactive glasses beyond bone and teeth: Emerging applications in contact with soft tissues, Acta Biomater., **2015**, 13, 1-15.
6- F. Baino, G. Novajra, V. Miguez-Pacheco, A. R. Boccaccini, C. Vitale-Brovarone, Bioactive glasses: Special applications outside the skeletal system, J. Non-Cryst. Solids, **2016**, 432, 15-30.
7- M. Cacciotti, M. Lombardi, A. Bianco, A. Ravaglioli, L. Montanaro, Sol-gel derived 45S5 bioglass: synthesis, microstructural evolution and thermal behavior, J. Mater. Sci.: Mater. Med., **2012**, 23, 1849-1866.
8- H. Zreiqat, C. R. Howlett, A. Zannettino, P. Evans, G. Schulze-Tanzil, C. Knabe, M. Shakibaei, Mechanisms of magnesium-stimulated adhesion of osteoblastic cells to commonly used orthopaedic implants, J. Biomed. Mater. Res., **2002**, 62, 175-184.
9- Y. Yamasaki, Y. Yoshida, M. Okazaki, A. Shimazu, T. Uchida, T. Kubo, Y. Akagawa, Y. Hamada, J. Takahashi, N. Matsuura, Synthesis of functionally graded $MgCO_3$ apatite accelerating osteoblast adhesion, J. Biomed. Mater. Res., **2002**, 62(1), 99-105.
10- R. K. Rude, H. E. Gruber, H. J. Norton, L. Y. Wei, A. Frausto, J. Kilburn, Dietary magnesium reduction to 25% of nutrient requirement disrupts bone and mineral metabolism in the rat, J. Bone, **2005**, 37, 211-219.
11- R. K. Rude, H. E. Gruber, L.Y. Wei, A. Frausto, B. G. Mills, Magnesium deficiency: effect on bone and mineral metabolism in the mouse, J. Calcif. Tissue Int., **2003**, 72, 32-41.
12- Q. Z. Chen, I. D. Thompson, A. R. Boccaccini, 45S5 Bioglass (R)-derived glass-ceramic scaffolds for bone tissue engineering, J. Biomater., **2006**, 27, 2414-2425.
13- H. D. Bao, Z. X. Guo, J. Yu, Effect of electrically inert particulate filler on electrical resistivity of polymer/multi-walled carbon nanotube composites, Polymer, **2008**, 49, 3826-3831.
14- S. W. Freiman, L. L. Hench, Kinetics of crystallization in Li_2O-SiO_2 glasses, J. Am. Ceram. Soc., **1968**, 51, 382-387.
15- R. A. J. Sambell, D. H. Bowen, D. C. Philips, Carbon fiber composites with ceramic and glass matrices, J. Mater. Sci., **1972**, 7, 663-666.
16- S. Chajri, S. Bouhazma, S. Herradi, H. Barkai, S. Elabed, S. Ibnsouda Koraichi, B. El Bali, M. Lachkar, Studies on preparation and characterization of SiO_2-CaO-P_2O_5 and SiO_2-CaO-P_2O_5-Na_2O bioglasses subtituted with ZnO, J. Mater. Environ. Sci., **2016**, 7(6), 1882-1897.
17- S. Bouhazma, S. Chajri, H. Barkai, S. Elabed, S. Ibnsouda Koraichi, B. El Bali, M. Lachkar, Synthesis, characterization, in vitro bioactivity and wettability of sol-gel derived SiO_2-CaO-P_2O_5 and SiO_2-CaO-P_2O_5-Na_2O bioglasses, Mor. J. Chem., **2015**, 3, 19-27.
18- I. Lebecq, F. Désanglois, A. Leriche, C. Follet-Houttemane, Compositional dependence on the in vitro bioactivity of invertor conventional bioglasses in the Si–Ca–Na–P system, J. Biomed. Mater. Res., **2007**, 83A, 156-168.
19- C. Duée, F. Désanglois, I. Lebecq, G. Moreau, A. Leriche, C. Follet-Houttemane, Mixture design applied to glass bioactivity evaluation in the Si–Ca–Na system, J. Non-Cryst. Solids, **2009**, 355, 943-950.

20- A. Tilocca, Models of structure, dynamics and reactivity of bioglasses: A Review, J. Mater. Chem., **2010**, 20, 6848-6858.
21- A. Saboori, M. Rabiee, F. Moztarzadeh, M. Sheikhi, M. Tahriri, M. Karimi, Synthesis, characterization and in vitro bioactivity of sol-gel derived SiO_2-CaO-P_2O_5-MgO bioglass, J. Mater. Sci. Eng., **2009**, C 29, 335-340.
22- T. Kokubo, H. Takadam, How useful is SBF in predicting in vivo bone bioactivity?, Biomaterials., **2006**, 27, 2907-2915.
23- ISO 23317, Implants for Surgery. In Vitro Evaluation for Apatite-forming Ability of Implant Materials., **2007**.
24- J. R. Jones, Review of bioactive glass: From Hench to hybrids, Acta Biomater., **2013**, 9, 4457-4486.
25- A. A. El-Rashidy, J. A. Roether, L. Harhaus, U. Kneser, A. R. Boccaccini, Regenerating bone with bioactive glass scaffolds: A review of in vivo studies in bone defect models, Acta Biomater., **2017**, 62, 1-28.
26- N. Li, R. Wang, Macroporous sol-gel bioglasses scaffold with high compressive strength, porosity and specific surface area, Ceramics International., **2012**, 38, 6889-6893.
27- Q. Z. Chen, G. A. Thouas, Fabrication and characterization of sol-gel derived 45S5 Bioglass-ceramic scaffolds, Acta Biomater., **2011**, 7, 3616-3626.
28- G. Arthur, Porosity and permeability changes during the sintering of copper powder, J. Inst. Met., **1955**, 83, 329-336.
29- S.Y. Ni, J. Chang, L. Chou, A novel bioactive porous $CaSiO_3$ scaffold for bone tissue engineering, J. Biomed. Mater. Res., 76, **2006**, 196-205.
30- A. B. Y. Hazar, Preparation and in vitro bioactivity of $CaSiO_3$ powders, Ceram. Int., **2007**, 33, 687-692.
31- I. Cacciotti, Bivalent cationic ions doped bioactive glasses: the influence of magnesium, zinc, strontium and copper on the physical and biological properties, J. Mater. Sci., **2017**, 52, 1-20.
31- E. Dietrich, H. Oudadesse, A. Lucas-Girot, M. Mami, In vitro bioactivity of melt derived glass 46S6 doped with magnesium, J. Biomed. Mater. Res., **2009**, 88A, 1087-1096.
32- I. Cacciotti, A. Bianco, High thermally stable Mg-substituted tricalcium phosphate via precipitation, Ceram. Int., **2011**, 37, 127-137.
33- I. Cacciotti, Cationic and anionic substitutions in hydroxyapatite, Handbook of Bioceramics and Biocomposites, Springer, **2016**, 145-211.
34- Y. Huang, X. G. Jin, X. L. Zhang, H. L. Sun, J. W. Tu, T. T. Tang, In vitro and in vivo evaluation of akermanite bioceramics for bone regeneration, Biomaterials, 30, **2009**, 5041-5048.
35- I. Cacciotti, M. Lombardi, A. Bianco, A. Ravaglioli, L. Montanaro, Sol-gel derived 45S5 bioglass: synthesis, microstructural evolution and thermal behaviour, J. Mater Sci: Materials in Medicine, **2012**, 23, 1849-1866.
36- A. Durif, Crystal Chemistry of Condensed Phosphates, Springer Science and Business Media, **2013**.
37- P. Li, I. Kangasniemi, K. de Groot, T. Kokubo, Bonelike hydroxyapatite induction by gel-derived titania on a titanium substrate, J. Am. Ceram. Soc., **1994**, 77, 1307-1312.
38- Q. Z. Chen, Li. Yuan, J. Li-Yu, M. W.Q, Julian, A. K. Paul, A new sol-gel process for producing Na_2O-containing bioactive glass ceramics, Acta Biomater., **2010**, 6, 4143-4153.
39- I. Cacciotti, G. Lehmann, A. Camaioni, A. Bianco, AP40 bioactive glass-ceramic by sol-gel synthesis: in vitro dissolution and cell-mediated bioresorption, Key Engineering Materials, **2013,** 541, 41-50.
40- L. C. Gerhardt, A. R. Boccaccini, Bioactive glass and glass-ceramic scaffolds for bone tissue engineering, Mater., **2010**, 3, 3867-3910.
41- F. Baino, E. Fiume, Elastic Mechanical Properties of 45S5-Based Bioactive Glass-Ceramic Scaffolds, Mater., **2019**, 12, 3244.
42- C. T. Wu, J. A. Chang, W. Y. Ni, S. Y. Zhai, J. Y. Wang, Porous akermanite scaffolds for bone tissue engineering: preparation, characterization, and in vitro studies, J. Biomed. Mater. Res. Part B, **2006**, 78, 47-55.
43- S. Callcut, J. C. Knowles, Correlation between structure and compressive strength in a reticulate glass-reinforced hydroxyapatite foam, J. Mater. Sci. Mater. Med., **2002**, 13, 485-489.